



## Electroless coating technology for 1060 aluminum alloy and the effect of tin chloride and polymer addition

A. M. Hewedy, O.R.M. Khalifa, A. A. Kassab, S. Y. Ahmed\*, M. M. Esmail  
 Faculty of Girls, Arts, Science and Education, Ain Shams University, Cairo, Egypt.



### Abstract

The protection of metals against corrosion is one of the most crucial roles played by deposited coatings. In our research, electroless coating of Al alloy 1060 by Ni-Sn-P deposit and Ni-Sn-Polymer composite. Firstly, we coat Al alloy 1060 with a Ni-P layer as a reference to our work. Then coat Al alloy 1060 with Ni-Sn-P coating by using different concentrations of tin chloride. The best alloy of Ni-Sn-P is then used to produce the quaternary Ni-Sn-polymer composite. Also, we use different concentrations of polyvinyl pyrrolidone (M.Wt. 40,000). By using a scanning electron microscope (SEM), their surface morphology and microstructure were examined. The composition of the coat was analyzed using thin film and EDAX analysis. The corrosion resistance was studied by potentiodynamic polarization in 3.5g/l sodium chloride solution. Corrosion protection is increased for the ternary alloy as tin increases, and the corrosion protection of the quaternary alloy increases as polymer content increases in the coated bath. The corrosion resistance sequence of the different used coats is Ni-Sn-polymer > Ni-Sn-P > Ni-P.

**Keywords:** Al 1060, Electroless, Coating, Ni-P, Ni-Sn-P, and Ni-Sn-PVP composite.

### 1. Introduction:

Surface engineering technology incorporates modifying solid surfaces. It can provide efficiency or additional characteristics, with surface coating. Metal industries use it a lot [1]. Electroless Ni-P coatings have become more common due to their good corrosion, abrasion and wear resistance [2–5]. Several studies have been made to enhance the corrosion characteristics of Ni-P alloy coatings on metal substrates [6–9]. The industry favored the electroless deposition due to homogeneous coating generation, which gives good adhesion to the substrate, and modified wear resistance, toughness and corrosion resistance properties [10]. Electrical conductivity, electro catalytic activity, corrosion resistance, mechanical characteristics, and crystalline [11] are all affected by the rate of phosphorus content in Ni-P coatings. Meanwhile, Ni-P films with low phosphorus content (3–5% P) have good corrosion resistance in concentrated sodium hydroxide solution, and Ni-P alloys with medium or high phosphorus content have excellent corrosion resistance in acidic solutions and in chloride medium [5,12,13]. Typically, to improve the qualities of the electroless binary Ni-P alloy, ternary Ni alloys were created using the co-deposition technology of Ni to give the ternary alloys, such as Ni – W – P [14,15], Ni – P – B [16–18], Ni – Fe – P [19–21], Ni – Cu – P [22–25], Ni – Co – P [26–29], Ni – Sn – P [30–35] and Ni For instance, studies have found that Ni – Sn – P alloys with low Sn content have good corrosion resistance. However, the majority of the work on Ni-based alloys was done at higher temperatures, such as 80–95 °C [36]. The effect of low tin additives on electroless Ni-P plating is investigated, with improved anticorrosion

performance reported in a 3.5 percent NaCl solution [37]. The Ni-Sn-P alloy coating was superior to the Ni-P alloy in terms of surface smoothness and corrosion resistance [38]. Many studies have shown that Ni–Sn–P alloys with a lower amount of Sn applied to them have better anti-corrosion properties than Ni–P deposits [32,39]. Due to their intrinsic stability, polymeric compounds can be used as acidic baths corrosion inhibitors [40,41]. PVP has attracted a lot of interest and has been used to suppress the corrosion of aluminum, iron, copper and low-carbon steel in a solution of hydrochloric acid, sulfuric acid, nitric acid, and phosphoric acid [42]. N-vinyl pyrrolidone monomers are linked together to form a long chain in polyvinyl pyrrolidone (PVP), which has a well-defined structure and is used as a surfactant, complexing agent, dispersant and stabilizer [43,44], a multipurpose added substance to enhance the reasonable and easy technique of electroless Ni-P alloy coatings since it has water solubility, biocompatibility, and non-toxicity [45]. The addition of Tin to the electroless Ni-P coating bath would be investigated in this work by studying its corrosion protection effect on the Al 1060 alloy. The basic technique of polarization analysis will be applied at room temperature, to obtain corrosion results.

### 2. Experimental:

#### a. Materials:

Al alloy 1060 of dimension (2.5 x 2 x 0.1cm<sup>3</sup>) and the composition of the alloy is shown in Table (1)

Al 1060 alloy specimens were chemically polished, degreased with an alkaline solution, rinsed with water and was dried before treatment. Electroless plating with Ni-Sn-

\*Corresponding author e-mail: [safaa.yhaia@women.asu.edu.eg](mailto:safaa.yhaia@women.asu.edu.eg); (Saffaa Yehia Ahmed).

Receive Date: 08 November 2023, Revise Date: 09 December 2023, Accept Date: 12 December 2023

DOI: 10.21608/EJCHEM.2023.245952.8835

©2024 National Information and Documentation Center (NIDOC)

P were produced by adding tin chloride to the original bath "Ni-P" using different concentrations of SnCl<sub>2</sub> (0.5, 0.66 and 1 g/l) to produce different alloys of Ni-Sn-P. Also, Ni-Sn-PVP composite were produced with adding different concentration of polyvinyl pyrrolidone (PVP) (5, 10 and 15g/L) on the Ni-Sn-P bath.

**Table (1): Chemical composition of aluminum 1060 (wt %).**

|         |         |         |         |
|---------|---------|---------|---------|
| Element | Si      | Fe      | Cu      |
| wt%     | 0.08635 | 0.33115 | 0.00119 |
| Element | Mn      | Mg      | Cr      |
| wt%     | 0.00297 | 0.00421 | 0.00030 |
| Element | Ni      | Zn      | Ti      |
| wt%     | 0.00187 | 0.00100 | 0.01295 |
| Element | Ag      | B       | Ba      |
| wt%     | 0.00023 | 0.00178 | 0.00010 |
| Element | Be      | Bi      | Ca      |
| wt%     | 0.00005 | 0.00100 | 0.00047 |
| Element | Cd      | Ce      | Co      |
| wt%     | 0.00021 | 0.00150 | 0.00050 |
| Element | Go      | Hg      | In      |
| wt%     | 0.01036 | 0.00100 | 0.00030 |
| Element | La      | Li      | Mo      |
| wt%     | 0.00030 | 0.00013 | 0.00050 |
| Element | Na      | P       | Pb      |
| wt%     | 0.00090 | 0.00100 | 0.00050 |
| Element | Sb      | Sn      | Sr      |
| wt%     | 0.00300 | 0.00192 | 0.00010 |
| Element | V       | Zr      | Sc      |
| wt%     | 0.01006 | 0.00093 | 0.05000 |

### b. Electroless Nickel process

#### i. Bath Composition:

A 100 ml glass beaker containing the electroless solution bath was maintained in a water bath system at a constant temperature of 85 °C. The pH that used for the coating bath is 8.5. All the deposits were plated for 20 minutes (after testing different times for coating, the best deposited times was obtained after 20 minutes). The bath used for the coating process is composed of 25 g/l nickel sulphate, 21 g/l sodium hypophosphite, 13 g/l tri-sodium citrates and 20 ml/l lactic acid. Ternary alloys Ni-Sn-P were obtained from the deposition of the original Ni-P bath containing different concentrations of tin chloride to give Ni-Sn-P (I, II and III). Also, Ni-Sn-PVP composite was obtained by adding different concentrations of PVP (5, 10 and 15g/L) to the Ni-Sn-P II bath to give Ni-Sn-PVP (I, II and III).

#### ii. Procedure:

Bath solution was kept at a constant temperature of 85°C throughout the electroless plating procedure, and reagent-grade reagents and purified water were used to prepare the solutions. The substrate was immersed in the absence and presence of tin chloride and polymer.

#### c. Properties of Electroless Deposition or layers:

Thermicostructure analysis was conducted with a scanning electron microscope model (Taiwan, Quanta 250 FEG), and thin film (x-ray

diffractometerPanalyticalcoX'pert PRO, Holland). Energy dispersive analysis of model ARL 9400 techniques has been applied to investigate the coatings phases structure and the composition of the coated films. Corrosion protection of different coatings was evaluated by potentiodynamic polarization using the CH Instrument CHI660D comprehensive electrochemical analyzers.

### 3. Result and discussion

#### a. Adhesion:

A thin diamond cutter was used to gently cut across the section of each specimen. On the mounted and polished section, the edge cut was examined first visually and then under a microscope. The results show that adhesion is improved when tin and PVP are present. This is a result of the interaction with the nickel, which enhances its substrate adhesive abilities.

#### i. Scanning electron microscope:

Figure 1(a-d) illustrates the surface morphology of binary Ni-P and ternary Ni-Sn-P alloys. There are nodules with the usual cauliflower-like appearance. This morphological observation indicated that the amount of Tin chloride in the plating bath affects the nucleation rate and deposit growth. With the addition of tin chloride from 0.50g/l to 0.66g/l, the surface morphology becomes more compact-grained and highly-coalescence smooth. The coat becomes unstable above 0.66 g/l (1.00 g/l). So, we ignore the addition of more than 0.66 g/L of tin chloride. We expect that the best ternary alloy is Ni-Sn-P II.

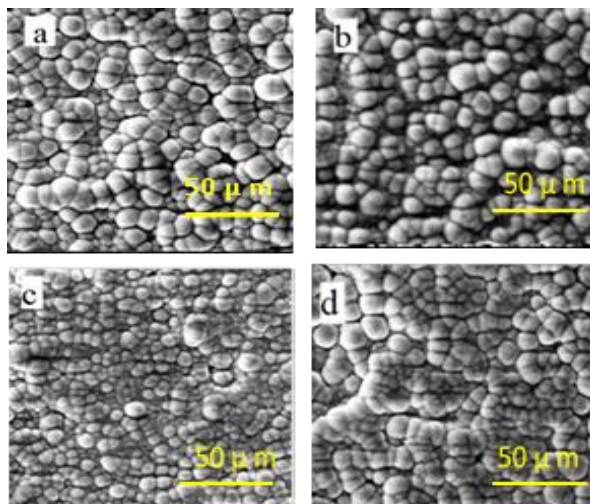


Fig.1. The surface morphology of (a) Ni-P (b) Ni-Sn-P I (c) Ni-Sn-P II and (d) Ni-Sn-P III.

Study the effect of polyvinyl pyrrolidone (PVP) in the same electroless bath (pH=8.5). We add different concentrations of PVP in the electroless Ni-Sn-P bath to form Ni-Sn-PVP I, Ni-Sn-PVP II and Ni-Sn-PVP III composites. The surface morphology of the quaternary Ni-Sn-polymer composites is in comparison with ternary Ni-Sn-P alloys. SEM micrographs of Ni-Sn-P, Ni-Sn-PVP I, Ni-Sn-PVP II and Ni-Sn-PVP III are shown in Fig. 2 (a-d). It can be seen that the coating shows a coarse nodular nanostructure. With increasing the polymer concentration in the electroless plating bath, a finer, more compact grain and strong coalescence were present in the surface morphology. With polymer composite, the nodules become smoother and finer.

### 3.2.1. Thin film:

The thin film layers of Ni-P, Ni-Sn-P I, Ni-Sn-P II and Ni-Sn-P III coatings are listed in Fig.3 (a- d). It's found that the structure of these types of coatings exhibits a nickel matrix in the range of  $2\theta$ , corresponding to 44.33. It is related to the III plane of the face centred cubic (FCC) phase of nickel. In our present investigation, the quantity of tin in a ternary alloy deposit is in solid solution forms since tin can only be dissolved in 19.3 weight percent nickel. So, the thin film of the ternary coatings revealed only a prominent Ni (III) peak. Small peaks at  $2\theta$  equal 44.33 reveal tin phosphide SnP hexagonal and also nickel phosphide Ni<sub>3</sub>P tetragonal observed.

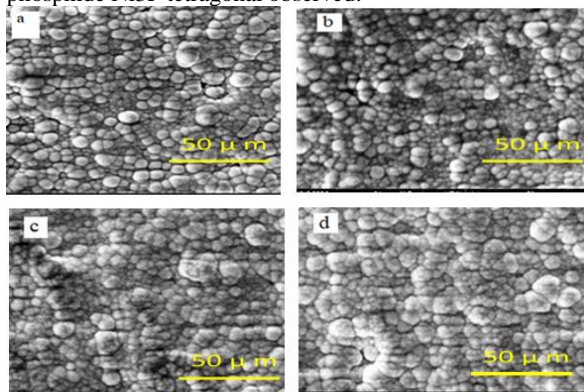


Fig.2. The surface morphology of (a) Ni-Sn-P (b) Ni-Sn-PVP I (c) Ni-Sn-PVP II and (d) Ni-Sn-PVP III.

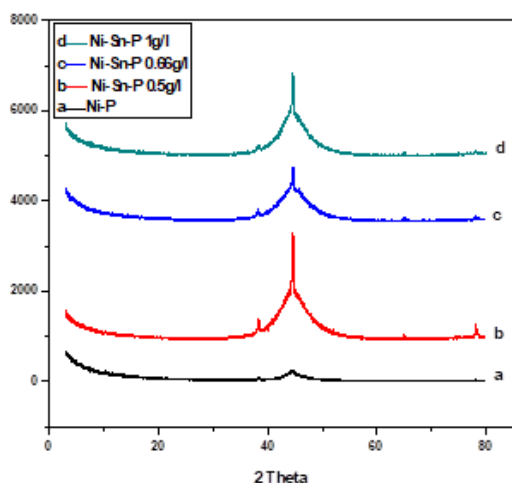


Fig.3. Thin film pattern of the as plated (a) Ni-P (b) Ni-Sn-P I (c) Ni-Sn-P II and (d) Ni-Sn-P III.

The calculated crystalline size using the Debye-Scherrer formula is listed in Table (2).

Table (2): Peak position ( $2\theta$ ) and crystallite size from (Debye-Scherrer formula for electroless Ni-P and Ni-Sn-P (I, II, III)).

| Type of coat | Peak position | Crystalline size (nm) |
|--------------|---------------|-----------------------|
| Ni-P         | 44.33         | 3.60                  |
| Ni-Sn-P I    | 44.33         | 5.50                  |
| Ni-Sn-P II   | 44.33         | 5.20                  |
| Ni-Sn-P III  | 44.33         | 5.80                  |

X-ray diffraction of the as-plated Ni-Sn-P, Ni-Sn-PVP I, Ni-Sn-PVP II and Ni-Sn-PVP III, respectively, is shown in Fig.4. (a-d). A single broad peak at  $2\theta$  equal 44.33 was present in every diffraction pattern. It is related to the face centred cubic (FCC) phase of nickel. The crystal microstructure of the composites is mainly amorphous. The crystalline size is shown in Table (3). The peak position and crystalline size from the Debye-Scherrer formula for Ni-Sn-P, Ni-Sn-PVP I, Ni-Sn-PVP II and Ni-Sn-PVP III are shown in Table (3)

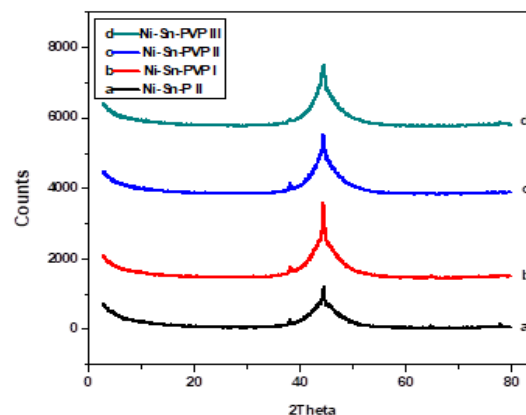


Fig.4. Thin film pattern of the as plated (a) Ni-Sn-P (b) Ni-Sn-PVP I (c) Ni-Sn-PVP II and (d) Ni-Sn-PVP III.

Table (3): Peak position and crystalline size from (Debye-Scherrer formula for electroless Ni-P and Ni-Sn-PVP (I, II, III))

| Type of coat  | Peak position | Crystalline size (nm) |
|---------------|---------------|-----------------------|
| Ni-Sn-P       | 44.33         | 5.20                  |
| Ni-Sn-PVP I   | 44.33         | 5.50                  |
| Ni-Sn-PVP II  | 44.33         | 5.60                  |
| Ni-Sn-PVP III | 44.33         | 5.90                  |

### b. EDX Analysis:

Element composition analysis carried out by EDX for the Ni-P and Ni-Sn-P alloys is given in Table (4). The binary alloy contains 89.01 Ni and 10.99 % P. For the ternary alloy Ni-Sn-P I, Ni-Sn-P II, and Ni-Sn-P III, the addition of Sn affected the percentage of nickel between 3 and 4 units of percentage, but had no effect on the phosphorous percentage, as shown in Table 4. Ni-Sn-P II with 85.95 % Ni, 2.15% Sn and 11.90 % P had the best corrosion protection because it had the largest percentage of Sn.

Table (4): Composition of as plated Ni-P, Ni-Sn-P I, Ni-Sn-P II and Ni-Sn-P III coatings determined by EDX analysis.

| Type of coat | Weight percent % |      |       |
|--------------|------------------|------|-------|
|              | Ni               | Sn   | P     |
| Ni-P         | 89.01            | ---- | 10.99 |
| Ni-Sn-P I    | 86.08            | 2.00 | 11.92 |
| Ni-Sn-P II   | 85.95            | 2.15 | 11.90 |
| Ni-Sn-P III  | 86.51            | 1.88 | 11.61 |

### c. Potentiodynamic polarization studies:

To understand the corrosion behavior of these coatings in detail, potentiodynamic polarization studies were performed in 3.5% NaCl solution at 30°C. Fig.5 (a - d) shows the polarization curves for binary and ternary coatings in 3.5% NaCl solution and are compared with 1060 Al alloy (dotted line). The electrochemical corrosion parameters obtained from the Tafel curves are tabulated in Table (5). It can be clearly seen from the table that the corrosion current density value for all the coatings in 3.5% NaCl solution ranges from  $5.557 \times 10^{-4}$  to  $1.1738 \times 10^{-4}$  nA/cm<sup>2</sup>. A higher corrosion current density value is obtained for

1060 Al alloy substrate ( $6.095 \times 10^{-4}$  nA/cm<sup>2</sup>). The calculated corrosion rate (mpy) for these coatings also shows a similar trend, as shown in Table (5).

It is evident from the literature on Ni-P coatings that preferential dissolution of nickel occurs, leading to the enrichment of phosphorous on the surface layer. This enriched phosphorous reacts with water to form

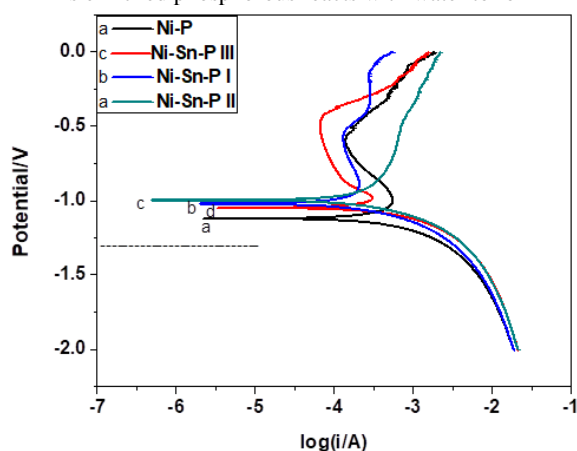


Fig.5. Potentiodynamic polarization curves of (a) Ni-P (b) Ni-Sn-P I (c) Ni-Sn-P II and (d) Ni-Sn-P III in 3.5%NaCl solution.

a layer of adsorbed hypophosphite anions ( $\text{H}_2\text{PO}_2^-$ ), this layer in turn blocks the supply of water to the electrode surface by preventing the hydration of nickel, which is considered to be the first step to form either  $\text{Ni}^{+2}$  species or a passive nickel film. Therefore, better corrosion resistance was obtained for electroless Ni-P and polyalloy coatings due to the enrichment of phosphorous on the electrode surface. The corrosion protection follows the sequence Ni-

Sn-P II < Ni-Sn-P I < Ni-Sn-P III < Ni- P.

Fig. (6) shows the potentiodynamic polarization curves for the 1060 Al substrate before and after coating with the best coat of Ni-Sn-P, i.e., Ni-Sn-P II, and the polymer coats Ni-Sn-PVP I, Ni-Sn-PVP II, and Ni-Sn-PVP III, all in 3.5% NaCl solution. The dotted line shows the polarization of the substrate in 3.5% NaCl. From the figure, it is observed that the presence of PVP on the all to alloy increases the passive region of the anodic curves and shifts to lower current density values. In addition, the corrosion potentials are shifted to less negative potentials as PVP increases in the coating bath, i.e., Ni-Sn-PVP III > Ni-Sn-PVP II > Ni-Sn-PVP I. The corrosion kinetic parameters determined from the polarization curves are listed in Table (6). The values of corrosion potential ( $E_{\text{corr}}$ ) increased with the presence of PVP in the coat Ni-Sn-P II at -0.996 V and Ni-Sn-PVP I at -0.618 V. At the same time, the corrosion current density ( $i_{\text{corr}}$ ) decreases with increasing PVP in the coat alloy. The corrosion current density for Ni-Sn-P II was  $1.1738 \times 10^{-4}$  nA/cm<sup>2</sup> and for Ni-Sn-PVP III was  $6.1105 \times 10^{-5}$  nA/cm<sup>2</sup>. The Quaternary alloy had the best corrosion protection because polyvinyl pyrrolidone had a high molecular weight and adhered to 1060 Al alloy. In addition, it is a nitrogen-containing compound that had excellent corrosion protective capacity because of the lone pair of electrons on the nitrogen atom. All the coats Ni-Sn-P II, Ni-Sn-PVP I, Ni-Sn-PVP II and Ni-Sn-PVP III had excellent corrosion resistance. corrosion protective capacity because of the lone pair of electrons on the nitrogen atom. All the coats Ni-Sn-P II, Ni-Sn-PVP I, Ni-Sn-PVP II and Ni-Sn-PVP III had excellent corrosion resistance.

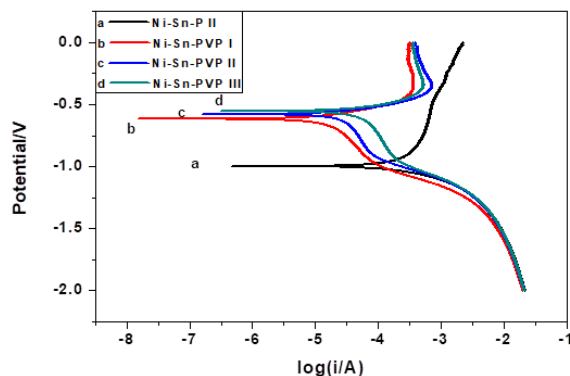


Fig.6. Potentiodynamic polarization curves of (a) Ni-Sn-P (b) Ni-Sn-PVP I (c) Ni-Sn-PVP II and (d) Ni-Sn-PVP III in 3.5% NaCl.

Table (5): Electrochemical data from Tafel curves carried out in 3.5%NaCl in presence of different concentration of tin chloride

| Type of coat   | $E_{\text{corr}}$ (volt) | $i_{\text{corr}}$ (nA/cm <sup>2</sup> ) | CR (mpy)               | Ba(V/dec) | Bc(V/dec) | Rp (ohm) |
|----------------|--------------------------|---|------------------------|-----------|-----------|----------|
| Uncoated alloy | -1.292                   | $6.095 \times 10^{-4}$                  | $7.984 \times 10^{-4}$ | 0.23      | 0.75      | 125.555  |
| Ni-P           | -1.122                   | $5.557 \times 10^{-4}$                  | $7.279 \times 10^{-4}$ | 0.25      | 0.78      | 148.125  |
| Ni-Sn-P III    | -1.053                   | $2.904 \times 10^{-4}$                  | $3.804 \times 10^{-4}$ | 0.33      | 0.81      | 351.05   |
| Ni-Sn-P I      | -1.018                   | $1.592 \times 10^{-4}$                  | $2.085 \times 10^{-4}$ | 0.52      | 0.87      | 888.867  |
| Ni-Sn-P II     | -0.996                   | $1.1738 \times 10^{-4}$                 | $1.537 \times 10^{-4}$ | 0.73      | 0.98      | 2264.858 |

Table (6): Electrochemical data from Tafel curves carried out in 3.5% NaCl for Ni-Sn-P, Ni-Sn-PVP I, Ni-Sn-PVP II and Ni-Sn-PVP III.

| Type of coat  | $E_{\text{corr}}$ (volt) | $I_{\text{corr}}$ (nA/cm <sup>2</sup> ) | $C_R$ (mpy)            | Ba(V/dec) | Bc(V/dec) | Rp(ohm)  |
|---------------|--------------------------|---|------------------------|-----------|-----------|----------|
| Ni-Sn-P II    | -0.996                   | 1.1738x10 <sup>-4</sup>                 | 1.537x10 <sup>-4</sup> | 0.73      | 0.98      | 2264.858 |
| Ni-Sn-PVP I   | -0.618                   | 9.0269x10 <sup>-5</sup>                 | 1.182x10 <sup>-4</sup> | 0.85      | 1.21      | 2404.753 |
| Ni-Sn-PVP II  | -0.592                   | 7.0843x10 <sup>-5</sup>                 | 9.280x10 <sup>-5</sup> | 0.97      | 1.44      | 3557.069 |
| Ni-Sn-PVP III | -0.557                   | 6.1108x10 <sup>-5</sup>                 | 8.005x10 <sup>-5</sup> | 1.08      | 1.64      | 4633.112 |

### Conclusion:

- Electroless deposition of a binary Ni-P alloy coating was deposited on 1060 Al alloy in an alkaline bath.
- Addition of Sn in the electroless Ni-P deposits resulted in a small effect in Ni% between 3 % and -4 %, with about no effect on P% content.
- All Ni-P, Ni-Sn-P I, Ni-Sn-P II, and Ni-Sn-P III have nanostructure with crystalline sizes of 3.6-5.8 nm. Ni-Sn-PVP I, Ni-Sn-PVP II, and Ni-Sn-PVP III had crystalline sizes of 5.2-5.9 nm
- Most of the obtained exhibited a spherical structure with compact and uniform grains and excellent adhesion to the substrate.
- All the deposits show good corrosion resistance in 3.5% NaCl solution.
- Our data indicate that corrosion protection should be applied in the following order:
- Ni-PVP III > Ni-PVP II > Ni-PVP I > Ni-Sn-P II > Ni-Sn-P I > Ni-Sn-P III > Ni-P.

### ACKNOWLEDGEMENTS

The authors gratefully thank Ain shams University, the Faculty of women, and the Chemistry Department

### Declaration of Competing Interests

The authors affirm that they have no known financial or interpersonal conflicts that might have appeared to have an impact on the research presented in this paper.

### References:

- [1] Singh G, Mohanty S, Kumar Singh R, Rai Dixit A, Kumar Sharma A. Comparative study on electroless composite coatings of textured and untextured Al-substrates. *Mater Today Proc* 2022. <https://doi.org/10.1016/j.matpr.2022.12.079>.
- [2] Ahmadi Ashtiani A, Faraji S, Amjad Iranagh S, Faraji AH. The study of electroless Ni-P alloys with different complexing agents on Ck45 steel substrate. *Arab J Chem* 2017;10:S1541–5. <https://doi.org/10.1016/j.arabjc.2013.05.015>.
- [3] Gao C, Dai L, Meng W, He Z, Wang L. Electrochemically promoted electroless nickel-phosphorous plating on titanium substrate. *Appl Surf Sci* 2017;392:912–9. <https://doi.org/10.1016/j.apsusc.2016.09.127>.
- [4] Omar R, El-sharief MA, Engineering M. OPTIMIZATION OF ELECTROLESS NI-P COATING BATH AND ITS IMPACT IN THE INDUSTRIAL 2021;49:42–52.
- [5] Shozib IA, Ahmad A, Abdul-Rani AM, Beheshti M,

Aliyu AA. A review on the corrosion resistance of electroless Ni-P based composite coatings and electrochemical corrosion testing methods. *Corros Rev* 2022;40:1–37. <https://doi.org/10.1515/corrrev-2020-0091>.

- [6] Abdel-Gawad SA, Sadik MA, Shoeib MA. Preparation and properties of a novel nano Ni-B-Sn by electroless deposition on 7075-T6 aluminum alloy for aerospace application. *J Alloys Compd* 2019;785:1284–92. <https://doi.org/10.1016/j.jallcom.2019.01.245>.
- [7] Tang SW, Wang CJ, Sun YL, Hu J. A study of corrosion resistance and formation characteristics of electroless Ni-P alloy coatings on Al18B4O33w/6061 Al composite with a simple surface pre-treatment. *Surf Coatings Technol* 2010;205:43–9. <https://doi.org/10.1016/j.surfcoat.2010.05.047>.
- [8] Gilberto D, Diaz A, Barba A, Jairo J, Florez O, Rafael J, et al. Effect of a Ni-P coating on the corrosion resistance of an additive manufacturing carbon steel immersed in a 0 . 1 M NaCl solution. *Mater Lett* 2020;275:128159. <https://doi.org/10.1016/j.matlet.2020.128159>.
- [9] Nazari H, Darband GB, Arefinia R. Review A review on electroless Ni – P nanocomposite coatings : effect of hard , soft , and synergistic nanoparticles. *J Mater Sci* 2023;58:4292–358. <https://doi.org/10.1007/s10853-023-08281-1>.
- [10] Sundararajan M, Devarajan M, Jaafar M. Electroless Ni-B sealing on nanoporous anodic aluminum oxide pattern: deposition and evaluation of its characteristic properties. *J Mater Res Technol* 2022;19:4504–16. <https://doi.org/10.1016/j.jmrt.2022.06.169>.
- [11] Bahramian A, Eyraud M, Vacandio F, Knauth P. Improving the corrosion properties of amorphous Ni-P thin films using different additives. *Surf Coatings Technol* 2018;345:40–52. <https://doi.org/10.1016/j.surfcoat.2018.03.075>.
- [12] Lin JD, Chou C Te. The influence of phosphorus content on the microstructure and specific capacitance of etched electroless Ni-P coatings. *Surf Coatings Technol* 2019;368:126–37. <https://doi.org/10.1016/j.surfcoat.2019.04.009>.
- [13] Shozib IA, Ahmad A, Majdi A, Tasnim N. Electroless Ni-P-TiO<sub>2</sub> (ENPT) Composite Coating: A Review on Microstructural Characteristics and Multifarious Properties for Surgical Instruments. *Solid State Technol* 2020;63:3989–96.
- [14] Li J, Wang D, Cai H, Wang A, Zhang J. Competitive

- deposition of electroless Ni-W-P coatings on mild steel via a dual-complexant plating bath composed of sodium citrate and lactic acid. *Surf Coatings Technol* 2015;279:9–15. <https://doi.org/10.1016/j.surfcoat.2015.08.017>.
- [15] Yang Y, Balaraju JN, Chong SC, Xu H, Liu C, Silberschmidt V V., et al. Significantly retarded interfacial reaction between an electroless Ni-W-P metallization and lead-free Sn-3.5Ag solder. *J Alloys Compd* 2013;565:11–6. <https://doi.org/10.1016/j.jallcom.2013.02.113>.
- [16] Shao QS, Bai RC, Tang ZY, Gao YF, Sun JL, Ren MS. Durable electroless Ni and Ni-P-B plating on aromatic polysulfonamide (PSA) fibers with different performances via chlorine-aided silver activation strategy. *Surf Coatings Technol* 2016;302:185–94. <https://doi.org/10.1016/j.surfcoat.2016.05.087>.
- [17] Wang Y, He J, Wang W, Shi J, Mitsuzaki N, Chen Z. Preparation and characterization of Ni-P/Ni 3.1 B composite alloy coatings. *Appl Surf Sci* 2014;292:462–8. <https://doi.org/10.1016/j.apsusc.2013.11.161>.
- [18] Lakavat M, Bhaumik A, Gandi S, Parne SR. Electroless Ni-P-B coatings on magnesium alloy AZ91D: influence of nano Al<sub>2</sub>O<sub>3</sub> on corrosion, wear, and hardness behaviour. *Surf Topogr Metrol Prop* 2022;10:25021.
- [19] Hou Y, Yuan Z, Yu X, Ma B, Zhao L, Kong D. Directly preparing well-dispersed ultra-hydrophilic NiFeP nanoparticle/Mxene complexes from spent electroless Ni plating solution as efficient hydrogen evolution catalysts. *J Environ Chem Eng* 2023;11:109738.
- [20] Wang L, Huang W, Huang G, Zhao L. Study of magnetic properties of Ni-Fe-P and Ni-Fe-P-B chemical films. *Int J Mater Res* 2022;93:298–302.
- [21] Wang H, Li W, Wu J, Wang D, Hou D, Sheng M, et al. Interface-Modified Ni-Fe-P/Co-P/NF Alloys for Electrocatalytic Water Splitting in Alkaline Solution. *Energy & Fuels* 2023.
- [22] Meng M, Leech A, Le H. Mechanical properties and tribological behaviour of electroless Ni-P-Cu coatings on corrosion-resistant alloys under ultrahigh contact stress with sprayed nanoparticles. *Tribol Int* 2019;139:59–66. <https://doi.org/10.1016/j.triboint.2019.06.031>.
- [23] Biswas P, Kalyan Das S, Sahoo P. Investigation of tribological and corrosion performance of duplex electroless Ni-P/Ni-Cu-P coatings. *Mater Today Proc* 2022. <https://doi.org/10.1016/j.matpr.2022.12.119>.
- [24] Biswas A, Das SK, Sahoo P. A comparative study in microstructural and tribological aspects of phosphorus enriched electroless Ni-P and Ni-P-Cu coating. *Mater Today Proc* 2019;19:403–8. <https://doi.org/10.1016/j.matpr.2019.07.625>.
- [25] Davoodi D, Emami AH, Vaghefi SMM, Omidi M, Bakhsheshi-Rad HR. Deposition of electroless Ni-Cu-P coatings on L80 steel substrates and the effects of coatings thickness and heat treatment on the corrosion resistance. *Int J Press Vessel Pip* 2022;200:104823.
- [26] Bi S, Zhao H, Hou L, Lu Y. Comparative study of electroless Co-Ni-P plating on Tencel fabric by Co 0 - based and Ni 0 -based activation for electromagnetic interference shielding. *Appl Surf Sci* 2017;419:465–75. <https://doi.org/10.1016/j.apsusc.2017.04.176>.
- [27] Battiatto S, Bruno L, Pellegrino AL, Terrasi A, Mirabella S. Optimized electroless deposition of NiCoP electrocatalysts for enhanced water splitting. *Catal Today* 2023;423:113929.
- [28] Wais AMH, AbidAli ARK. Studying the behavior of Ni-Co-P and Ni-Co-P-B4c electroless coatings and heat treatment on mechanical and corrosion properties of AISI 4140 steel. *AIP Conf. Proc.*, vol. 2787, AIP Publishing; 2023.
- [29] Jafari R, Ahmadi NP, Khosroshahi RA, Raghebi Z. DEPOSITING Ni-Co-P ALLOY COATING ON AISI316 STEEL AND ANALYZING ITS PROPERTIES. *Surf Rev Lett* 2023;30:2350005.
- [30] Zhang WX, Jiang ZH, Li GY, Jiang Q, Lian JS. Electroless Ni-Sn-P coating on AZ91D magnesium alloy and its corrosion resistance. *Surf Coatings Technol* 2008;202:2570–6. <https://doi.org/10.1016/j.surfcoat.2007.09.023>.
- [31] Gunji T, Umehashi Y, Tsunoi H, Yokoi K, Kawai A, Matsumoto F. Preparation of chemical-resistant atomically ordered Sn-Ni alloy films by electroless plating. *J Alloys Compd* 2021;877:160100. <https://doi.org/10.1016/j.jallcom.2021.160100>.
- [32] Wang Y, Tang R, Yang C, Xu T, Mitsuzaki N, Chen Z. Effect of sodium stannate on low temperature electroless Ni-Sn-P deposition and the study of its mechanism. *Thin Solid Films* 2019;669:72–9. <https://doi.org/10.1016/j.tsf.2018.10.038>.
- [33] Chen B, Xie H, Shen L, Xu Y, Zhang M, Yu H, et al. Electroless Ni-Sn-P plating to fabricate nickel alloy coated polypropylene membrane with enhanced performance. *J Memb Sci* 2021;640:119820. <https://doi.org/10.1016/j.memsci.2021.119820>.
- [34] Tsunoi H, Shimizu M, Aoyagi H, Mizushima M, Kawai A, Fukunishi M, et al. Chemical Resistance Property of Electroless Deposited Ni-Sn-P Layers Having High Sn Content. *ACS Sustain Chem Eng* 2023.
- [35] Fu A, Li F, Yang Y, Zhang H, Li L, Miao J, et al. Corrosion mechanism of electroless Ni-Sn-P coating in multi thermal fluid. *Mater Res Express* 2019;6:126424.
- [36] Zhao G, Zou Y, Zhang H, Zou Z. Correlation between corrosion resistance and the local atomic structure of electroless, annealed Ni-P amorphous alloys. *Mater Lett* 2014;132:221–3. <https://doi.org/10.1016/j.matlet.2014.06.081>.
- [37] Popoola API, Loto CA, Osifuye CO, Aigbodion VS, Popoola OM. Corrosion and wear properties of Ni-Sn-P ternary deposits on mild steel via electroless method. *Alexandria Eng J* 2016;55:2901–8. <https://doi.org/10.1016/j.aej.2016.06.018>.
- [38] Liu C, Gan X. Microstructure and properties of open-cell Ni-Sn-P alloy foams prepared by electroless plating. *Surf Coatings Technol* 2020;924–30. <https://doi.org/10.1002/maco.201911388>.
- [39] Liu W, Xu DD, Duan XY, Zhao GS, Chang LM, Li X. Structure and effects of electroless Ni-Sn-P transition layer during acid electroless plating on

- magnesium alloys. *Trans Nonferrous Met Soc China* (English Ed 2015;25:1506–16. [https://doi.org/10.1016/S1003-6326\(15\)63752-9](https://doi.org/10.1016/S1003-6326(15)63752-9).
- [40] Benchadli A, Attar T, Messaoudi B, Choukchou-Braham E. Polyvinylpyrrolidone as a Corrosion Inhibitor for Carbon Steel in a Perchloric Acid Solution: Effect of Structural Size. *Hungarian J Ind Chem* 2021;49:59–69. <https://doi.org/10.33927/hjic-2021-08>.
- [41] Khamis EA, Hamdy A, Morsi RE. Magnetite nanoparticles/polyvinyl pyrrolidone stabilized system for corrosion inhibition of carbon steel. *Egypt J Pet* 2018;27:919–26. <https://doi.org/10.1016/j.ejpe.2018.02.001>.
- [42] Schweinsberg DP, Jianguo Y, Lin W, Otienoalego V. Polyvinylpyrrolidone and polyethylenimine as inhibitors for the corrosion of a low carbon steel in phosphoric acid. *Corros Sci* 1995;37:975–85.
- [43] Yang C-C, Wan C-C, Wang Y-Y. The Role of Poly(N-vinyl-2-pyrrolidone) in AgPd Nanoparticles Formation and Its Application to Electroless Deposition. *J Electrochem Soc* 2006;153:J27. <https://doi.org/10.1149/1.2176917>.
- [44] Al Juhaiman LA. Polyvinyl pyrrolidone as a corrosion inhibitor for carbon steel in HCl. *Int J Electrochem Sci* 2016;11:2247–62.
- [45] Guo SQ, Hou LF, Guo CL, Wei YH. Characteristics and corrosion behavior of nickel-phosphorus coatings deposited by a simplified bath. *Mater Corros* 2017;68:468–75. <https://doi.org/10.1002/maco.201609155>.